Recombination of W^{19+} ions with electrons: Absolute rate coefficients from a storage-ring experiment and from theoretical calculations

N. R. Badnell,[1,*] K. Spruck,[2,3] C. Krantz,[3] O. Novotný,[4] A. Becker,[3] D. Bernhardt,[2] M. Grieser,[3] M. Hahn,[4] R. Repnow,[3] D. W. Savin,[4] A. Wolf,[3] A. Müller,[2] and S. Schippers[2,5]

[1]*Department of Physics, University of Strathclyde, Glasgow G4 0NG, United Kingdom*
[2]*Institut für Atom- und Molekülphysik, Justus-Liebig-Universität Gießen, Leihgesterner Weg 217, 35392 Giessen, Germany*
[3]*Max-Planck-Institut für Kernphysik, Saupfercheckweg 1, 69117 Heidelberg, Germany*
[4]*Columbia Astrophysics Laboratory, Columbia University, 550 West 120th Street, New York, New York 10027, USA*
[5]*I. Physikalisches Institut, Justus-Liebig-Universität Gießen, Heinrich-Buff-Ring 16, 35392 Giessen, Germany*

Experimentally measured and theoretically calculated rate coefficients for the recombination of $W^{19+}([Kr]\,4d^{10}\,4f^9)$ ions with free electrons (forming W^{18+}) are presented. At low electron-ion collision energies, the merged-beam rate coefficient is dominated by strong, mutually overlapping, recombination resonances as already found previously for the neighboring charge-state ions W^{18+} and W^{20+}. In the temperature range where W^{19+} is expected to form in a collisionally ionized plasma, the experimentally derived recombination rate coefficient deviates by up to a factor of about 20 from the theoretical rate coefficient obtained from the Atomic Data and Analysis Structure database. The present calculations, which employ a Breit–Wigner redistributive partitioning of autoionizing widths for dielectronic recombination via multi-electron resonances, reproduce the experimental findings over the entire temperature range.

I. INTRODUCTION

Tungsten will be the material of choice for critical components of the International Thermonuclear Experimental Reactor (ITER) fusion reactor, including parts of the inner wall as well as the divertor [1]. Tungsten ions will be present as impurities in the fusion plasma by physical sputtering or evaporation. The charge balance of tungsten ions in a nonequilibrium plasma has large uncertainties covering many charge states relevant to fusion [2]. To model it, rate coefficients for charge-changing collision processes such as electron-impact ionization [3] and electron-ion recombination [2] are required. This latter work [2] is part of a new effort to calculate partial and total recombination rate coefficients for the entire tungsten isonuclear sequence for use in collisional-radiative modeling. In addition, to guide the development of the theoretical methods and to be able to assess the associated uncertainties, we have set out to provide experimental benchmarks for the recombination of the particularly complex open-$4f$-shell tungsten ions. So far, we have reported results for W^{18+} and W^{20+} [4–7]. The main finding has been a much larger measured recombination rate coefficient than was initially expected theoretically, and which is still used in the Atomic Data and Analysis Structure (ADAS) database [8] for plasma modeling. Theoretically, this difference has been described by a Breit–Wigner redistribution of the initial dielectronic capture so as to model the population of highly mixed multiply excited electron states [5,9] and, most recently, by allowing for nonunit fluorescence yields [7,10]. The current interest is to see how results and comparisons change as we move from one open-f-shell ion to the next.

Here, we present experimental and theoretical results for the recombination of $W^{19+}([Kr]\,4d^{10}\,4f^9)$ ions with free electrons. This work is part of an extended research project in which the photoionization, electron-impact ionization, and electron-ion recombination of tungsten ions is investigated [11]. The experimental and theoretical methodology used here has already been described in detail in a preceding publication [7] on the recombination of $W^{18+}([Kr]\,4d^{10}\,4f^9)$, where further references to related work can be found also. Here, we briefly discuss only those experimental (Sec. II) and theoretical (Sec. III) aspects which are specific for the W^{19+} primary ion under study. The results are presented and discussed in Sec. IV. A summary of the work and findings is given in Sec. V.

II. EXPERIMENT

The electron-ion merged-beams technique was applied at the test storage ring (TSR) heavy-ion storage ring of the Max-Planck-Institut für Kernphysik (MPIK) in Heidelberg, Germany. Mass-to-charge ratio selected $^{182}W^{19+}$ ions with a kinetic energy of $\sim186\,\text{MeV}$ were supplied by the MPIK accelerator facility. The TSR electron cooler was used for electron cooling of the stored W^{19+} ion beam and as an electron target for the present recombination measurements. At the beginning of each measurement cycle W^{19+} ions were injected into the storage ring and first cooled for 1.5 s with the cooler cathode voltage adjusted to match electron and ion velocities. The 1.5 s cooling time also allowed for the decay of the metastable W^{19+} ions (see below) that were populated in the foil-stripping processes which were used both inside and behind the accelerator to produce the desired primary ion charge state.

For the measurement of the W^{19+} recombination rate coefficient, the count rate of W^{18+} product ions was recorded as a function of electron-ion collision energy. As in our previous recombination experiments with W^{20+} [4] and W^{18+} [7] ions, the resulting relative merged-beam recombination rate

*[*]badnell@phys.strath.ac.uk

TABLE I. W^{19+} levels from the [Kr]$4d^{10}4f^9$, [Kr]$4d^{10}4f^85s$, and [Kr]$4d^{10}4f^85p$ configurations with predicted lifetimes longer than 20 ms. E_{ex} is the calculated excitation energy from the [Kr]$4d^{10}4f^9$ $^6H_{15/2}$ ground level. Numbers in brackets denote powers of ten.

E_{ex} (eV)	Level	Lifetime (s)
0	$4f^9$ $^6H_{15/2}$	∞
2.114	$4f^9$ $^6H_{11/2}$	1.54[−1]
2.523	$4f^9$ $^6F_{9/2}$	8.88[+1]
2.588	$4f^9$ $^6F_{11/2}$	4.17[−2]
2.979	$4f^9$ $^6H_{9/2}$	3.53[−2]
3.422	$4f^9$ $^6H_{7/2}$	4.90[−2]
3.602	$4f^9$ $^6F_{7/2}$	4.57[−2]
3.839	$4f^9$ $^6H_{5/2}$	2.83[−1]
4.178	$4f^9$ $^6F_{3/2}$	3.48[+1]
4.524	$4f^9$ $^6F_{1/2}$	3.41[−1]
6.025	$4f^9$ $^4M_{21/2}$	∞[a]
6.065	$4f^9$ $^4K_{17/2}$	4.23[−2]
6.343	$4f^9$ $^4L_{19/2}$	2.31[+0]
12.117	$4f^9$ $^2O_{23/2}$	4.78[−2]
28.278	$4f^8 5s$ $^4O_{25/2}$	6.39[−2]

[a]The ($M3$) lifetime is of the order of the age of the universe.

coefficient (after background subtraction) was normalized to the recombination rate coefficient α_0 at 0 eV average electron-ion collision energy. For W^{19+} we deduced $\alpha_0 = 2.0 \times 10^{-6}$ cm^3/s from the storage lifetime of the W^{19+} ion beam.

The experimental energy spread and the uncertainty of the experimental energy scale are the same as in our previous experiment with W^{18+} ions [7], which was carried out under the same conditions of and immediately before the present measurements. At a confidence limit of 90%, the statistical error of the absolute rate coefficient at zero collision energy amounts to 6%. The total uncertainty of the data at a 90% confidence limit, i.e., the quadrature sum of systematic [7] and statistical uncertainty, ranges from 9% at 0 eV across 11% at 1 eV, 16% at 30 eV and 155% at 150 eV, as the rate coefficient approaches zero. These errors stem from data reduction only and do not take into account any uncertainties due to the presence of stored ions in excited long-lived metastable levels.

For an estimate of the metastable fractions in the cooled ion-beam, lifetimes of metastable levels of the W^{19+} ground configuration [Kr]$4d^{10}4f^9$ and of the first-excited configurations [Kr]$4d^{10}4f^85s$ and [Kr]$4d^{10}4f^85p$ were calculated with the AUTOSTRUCTURE atomic code [12]. In the calculation, the ground level is found to be [Kr]$4d^{10}4f^9$ $^6H_{15/2}$, as predicted earlier [13]. In addition, there are 2468 excited levels within the chosen set of electron configurations. Their excitation energies range up to about 129 eV above the ground level. Their lifetimes were determined by calculating $E1$, $M1$, and $E2$ radiative transition rates to all accessible energetically lower states. The results for all levels with lifetimes longer than 20 ms can be found in Table I. According to our calculations there are four excited levels with radiative lifetimes above one second.

All calculated transition rates were used to simulate the level populations in the stored W^{19+} beam as a function of storage time. To this end, a set of coupled rate equations [14]
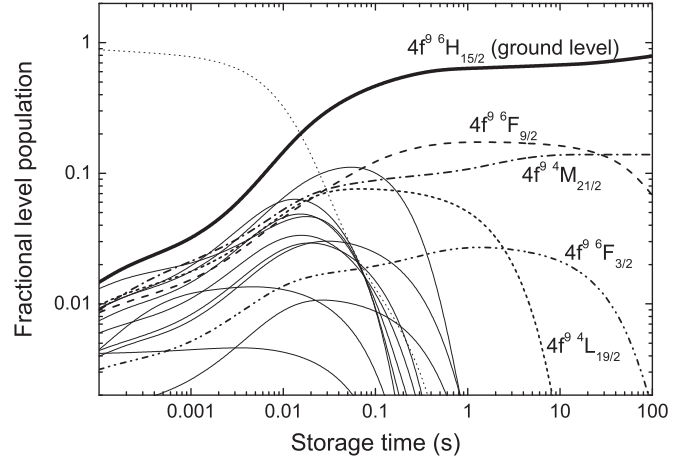

FIG. 1. Populations of the 2469 levels of the [Kr]$4d^{10}4f^9$ ground configuration and the [Kr]$4d^{10}4f^85s$ and [Kr]$4d^{10}4f^85p$ first excited configurations of W^{19+} as a function of ion storage time. The thick solid line represents the population of the [Kr]$4d^{10}4f^9$ $^6H_{15/2}$ ground level, the dashed, dash-dotted, dash-dot-dotted, and short-dashed lines denote the populations of the long-lived metastable [Kr]$4d^{10}4f^9$ $^6F_{9/2}$, $^4M_{21/2}$, $^6F_{3/2}$, and $^4L_{19/2}$ levels, respectively. The thin solid lines represent the remaining 10 levels from Table I. The dotted line represents the sum of the populations of the 2554 short-lived levels, which are not listed in Table I.

has been solved numerically. As an initial condition, a Boltzmann distribution with a temperature of 560 eV, corresponding to the effective energy of the electrons in the stripping foil, has been assumed to estimate the level populations [14]. Figure 1 shows the resulting populations as a function of storage time. After 1.5 s about 64% of the stored ions have decayed to the ground level and 17%, 11%, 5%, and 3% have been accumulated in the long-lived metastable [Kr]$4d^{10}4f^9$ $^6F_{9/2}$, $^4M_{21/2}$, $^4L_{19/2}$, and $^6F_{3/2}$ levels, respectively. This result is largely independent of the temperature used to characterize the Boltzmann distribution of initial level populations. This beam composition did not change significantly during the measurement time interval of $\sim$2 s duration that followed the 1.5 s cooling period.

Such population modeling likely provides only an upper estimate of the metastable fraction since other factors such as collisions, Stark mixing, etc. can quench excited states. When the metastable fraction is modest, say less than 10%, its possible effect can be neglected since it is small compared to other experimental uncertainties. However, the present estimate of a 36% metastable fraction requires some theoretical investigation, which we discuss next.

III. THEORY

Our calculational approach closely follows that used for W^{18+} [7] and is initially based on the independent processes isolated resonance using distorted waves (IPIRDW) approximation. We used the program AUTOSTRUCTURE [12] to calculate all relevant energy levels, radiative rates, and autoionization rates necessary to describe the full range of two-step dielectronic-recombination (DR) reactions which take place via $\Delta n = 0$ and $\Delta n = 1$ promotions of $4d$ and

$4f$ electrons from the W^{19+} ground state. Previously, we used configuration-average (CA), LS-, and intermediate-coupling schemes. We found no advantage to using intermediate coupling, and it is computationally demanding. Thus, for the total DR rate coefficient, summed over $\Delta n = 0$ and $\Delta n = 1$ promotions, we restrict ourselves to using the CA approximation.

Basic IPIRDW DR results fall far short of experiment [5]. Even in intermediate coupling, use of the above limited configuration interaction expansion does not take account of mixing (in CA there is none) with the many complex, multiply excited states which lie near threshold. Consequently, these states are not populated by dielectronic capture in such an approximation. Nevertheless, they could easily radiatively stabilize if populated and greatly increase the low-energy DR cross section. A simple Breit–Wigner redistribution of the IPIRDW autoionization rates (with unit fluorescence yield) gave a factor-of-three increase in the DR cross section of W^{20+} [5,9].

This simple approach breaks down as the scattering energy increases and more autoionizing channels open up. Subsequently, use of nonunit fluorescence yields modeled the rapid falloff of the DR cross section with increasing energy, for W^{20+} [10] and W^{18+} [7]. As discussed in Ref. [7], we again use a dimensionless Breit–Wigner weighting (of width 10 eV) to redistribute our autoionizing widths over an arbitrary but uniform partitioning of autoionizing energies. The characteristic radiative widths are taken to be those associated with the initial capture. We again find little difference if we redistribute the autoionization widths across many multiply excited configurations and then use their respective radiative widths. The basic reason for this, of course, is the fact that complete redistributive mixing leads to a regime where the DR cross section is proportional to the redistributed autoionizing widths and so is independent of the actual unitary redistribution function [5].

The theoretical merged-beam recombination rate coefficient is obtained by convoluting these theoretical cross sections with a flattened Maxwellian electron velocity distribution [15] with the temperatures $k_B T_\parallel = 0.2$ meV and $k_B T_\perp = 20$ meV. The TSR dipole magnets field ionize the weakly bound high-n Rydberg levels of the recombined W^{18+} ion before they can be detected. The critical principal quantum number for field ionization in this experiment is $n_{\max} = 69$ [16]. This cutoff quantum number was used for all theoretical merged-beam rate coefficients.

Regarding metastables: DR from excited levels in simple systems is normally strongly suppressed at all energies compared with that from the ground level. This is due to autoionization into the continuum of levels which lie below the initial metastable level. As we have seen, the DR of the open f shell is a very different problem. In order to investigate the dependence of DR on the initial *level* we carried out full intermediate-coupling DR calculations with Breit–Wigner redistribution and damping, as we did previously for W^{18+} [7], but restricted to the $\Delta n = 0$ contribution so as to keep the problem tractable. We note that $\Delta n = 0$ contributes roughly a third to a half of the theoretical total. Results for the lowest 16 initial levels are shown in Fig. 2. The ground and the long-lived $^4 M_{21/2}$ levels are highlighted. Above $\sim$20 eV, there is a spread
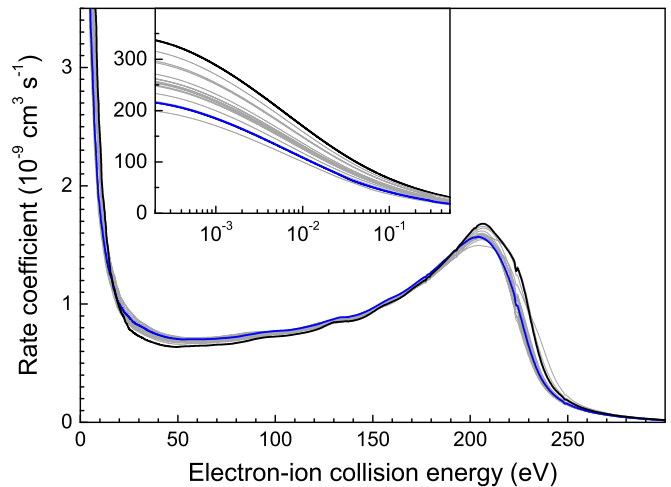

FIG. 2. Partitioned-damped intermediate coupling rate coefficients for electron-ion recombination of W^{19+}, via $\Delta n = 0$ promotions of $4d$ and $4f$, for the lowest 16 initial levels. The ground level curve is highlighted in black—it is the uppermost curve in the inset and at the peak at 200 eV—as is the long-lived $^4 M_{21/2}$ level, in blue.

of only $\sim$10%, until above $\sim$200 eV, where the rate coefficient falls off rapidly. Below $\sim$20 eV, the rate coefficient rises rapidly. At the lowest energies, below $\sim$0.1 eV, the long-lived $^4 M_{21/2}$ result is about two-thirds that of the ground level. Thus, and given the upper estimate nature of the metastable fraction, we do not feel justified in making any adjustments to either the theoretical or measured rate coefficients. Strictly speaking, our comparison of theory and experiment that follows is valid for a negligible metastable fraction, or DR from the metastables differing little from the ground level.

IV. RESULTS

The measured and calculated merged-beam recombination rate coefficients of W^{19+} are displayed in Fig. 3 over the energy range 0 to 300 eV. In the collision-energy range of 0 to about 5 eV the rate coefficient decreases from a value of $\alpha_0 = 2.0 \times 10^{-6}$ cm^3/s by approximately two orders of magnitude. At higher energies, almost up to the end of the experimental energy range, broad resonance structures are visible. Since their widths are larger than the experimental energy spread, these features are most likely blends of unresolved resonances. The rise of the measured rate coefficient at energies below $\sim$0.5 meV is an experimental artifact [17] which is disregarded in the comparisons with the present theoretical calculations and in the derivation of the experimentally derived plasma rate coefficient below.

The inset in Fig. 3 enlarges the low-energy region. Up to at least 1 eV, the calculated radiative-recombination (RR) rate coefficient is always more than two orders of magnitude smaller than the experimental data. This indicates that the measured rate coefficient is dominated by strong contributions from resonant processes. Over the experimental collision-energy range, our partitioned damped (PD) results are in satisfying agreement—given the complexity of the computational problem—with the measured rate coefficient, although they do not reproduce the dip in the experiment over
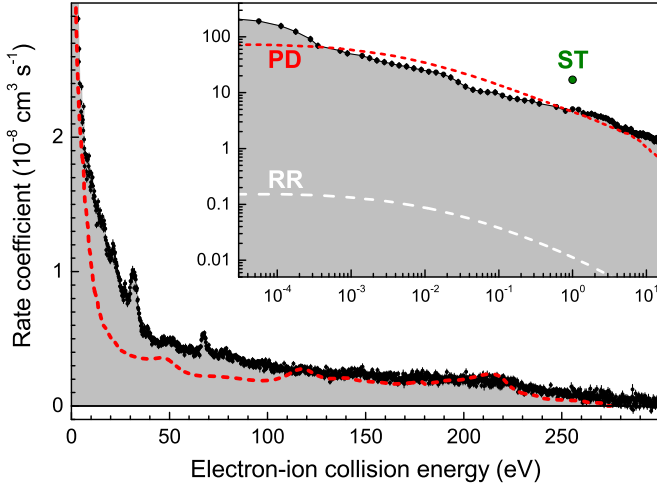
FIG. 3. Comparison of our measured (symbols) and various calculated merged-beam recombination rate coefficients. The short-dashed line (labeled PD) is the result of the fully partitioned calculation including autoionizing and radiative damping. The long-dashed line (labeled RR) is the calculated rate coefficient for radiative recombination. The inset shows the same data on a double logarithmic scale. The full circle (labeled ST) is the rate coefficient from the statistical theory by Dzuba *et al.* [9].

0.03 to 0.8 eV. The rapid falloff to 5 eV is mirrored well. Then, up to about 110 eV, the experimental rate coefficient exhibits a more pronounced resonance structure than the calculated one. At even higher energies both experiment and PD theory almost coincide up to the $4d$–$4f$ limit, ending at about 280 eV. The $4f$–$5l$ limit at about 215 eV is more clearly visible in the calculation than in the experiment.

The experimentally derived plasma recombination rate coefficient is obtained from the measured merged-beam recombination rate coefficient essentially by first converting it into a cross section which is then convoluted with an isotropic Maxwellian energy distribution characterized by the plasma electron temperature T_e [16]. Figure 4 shows the plasma recombination rate coefficient derived from the experimental merged-beam recombination rate coefficient for W^{19+} forming W^{18+}, as well as several theoretical results. The plasma temperature range where the abundance of this charge state is expected to peak in a fusion plasma is indicated by the shaded area. At a plasma temperature of 1 eV the experimentally derived rate coefficient is about 5×10^{-8} cm^3/s. Towards higher temperatures it decreases monotonically by more than two orders of magnitude over the displayed temperature range. At temperatures above about 250 eV, the present result is to be regarded as a lower limit, since it does not contain any contribution from recombination at electron-ion collision energies above 300 eV. Theoretically, we estimate the missing contribution, from all resonances which lie above 300 eV and those below 300 eV with principal quantum number $n > 69$, to be less than 5% at 1000 eV. This amount decreases with decreasing temperature until low temperatures where the high-n RR contribution starts to rise again, but it is still no more than 1% at 1 eV. The systematic and statistical uncertainties of the experimental merged-beam recombination rate coefficient (Sec. II) leads to an uncertainty in the plasma rate coefficient.
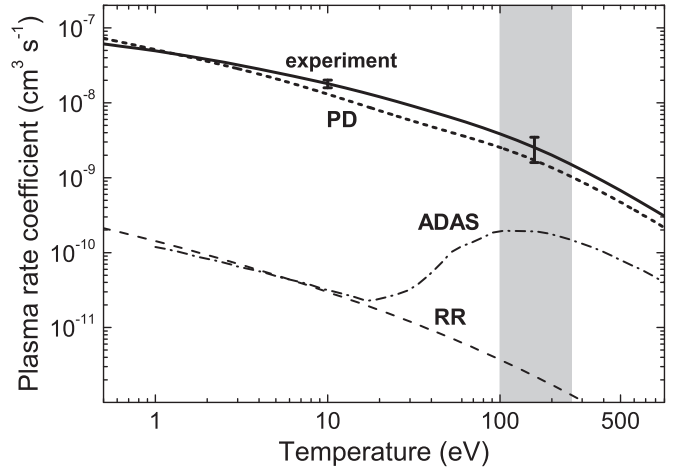

FIG. 4. Experimentally derived (thick solid line) and theoretical rate coefficients for electron-ion recombination of W^{19+} in a plasma. The error bars represent the combined statistical and systematic uncertainty (see text) of the experimentally derived rate coefficient. The short-dashed line (labeled PD) is the result of the present partitioned-and-damped theory. The dash-dotted line is the plasma recombination rate coefficient from the ADAS database [8,18]. The long-dashed line is the calculated RR plasma rate coefficient. The shaded area indicates the plasma temperature range where W^{19+} is expected to form in a collisionally ionized plasma [19].

At a 90% confidence limit, the total relative uncertainty of the experimentally derived rate coefficient, including the missing resonance strength from high-n states, is estimated to be 37% at a temperature of 150 eV. In the same way we obtain a total uncertainty of 12% at a temperature of 10 eV. These uncertainties are similar to what was obtained for W^{18+} [7]. The experimental plasma rate coefficients can be conveniently expressed by a simple fit formula [Eq. (3) of Ref. [7]]. The fit coefficients in Table II are valid for the temperature range 1–1000 eV.

The PD result agrees with the experimentally derived rate coefficient within the experimental uncertainties; in particular, over the temperature range ~100–260 eV where W^{19+} is expected to form in a collisionally ionized plasma [19]. At lower temperatures between about 5 and 100 eV, the theoretical plasma rate coefficient is slightly smaller than the experimental one. This is due to the underestimation by the PD theory of

TABLE II. Best-fit parameters for Eq. (3) of Ref. [7], reproducing the experimentally derived plasma recombination rate coefficient (Fig. 4) with less than 2% relative deviation for temperatures $1 \text{ eV} \leqslant k_B T \leqslant 1000 \text{ eV}$, with k_B denoting the Boltzmann constant.

i	c_i (cm^3 s^{-1} K$^{3/2}$)	E_i (eV)
1	0.07856	0.55162
2	0.28403	2.8647
3	0.68293	9.0733
4	1.4833	23.545
5	2.5401	59.832
6	4.0871	137.32
7	2.6149	239.36

the DR resonance strength at electron-ion collision energies 5–110 eV (Fig. 3 and discussion above).

The DR contribution to the recombination rate coefficient from the ADAS database [8,18] was calculated by using the Burgess general formula [20]. The general formula is a high-temperature approximation and contains no description of low-energy resonances or low-temperature DR. At low plasma temperatures, the ADAS rate coefficient is due purely to radiative recombination and so decreases monotonically up to about 20 eV. In this temperature range it is more than two orders of magnitude lower than the experimentally derived plasma rate coefficient.

Resonances lead to the rise of the ADAS rate coefficient at temperatures above 20 eV. The ADAS rate coefficient reaches its maximum at 105 eV where it is a factor of ∼20 lower than the experimentally derived rate coefficient. This factor varies from 20 to 18 over the key plasma temperature range ∼100–260 eV.

V. SUMMARY

Rate coefficients for the recombination of W^{19+}([Kr]$4d^{10}4f^9$) ions with free electrons have been obtained independently on absolute scales from a storage-ring experiment and from theoretical calculations. The experimental rate coefficient is dominated by particularly strong recombination resonances at very low electron-ion collision energies; below about 10 eV. These resonances significantly influence the W^{19+} recombination rate coefficient in a plasma even at temperatures of 100–260 eV where W^{19+} is expected to form in a collisionally ionized plasma. These experimental findings for W^{19+} are very similar to the results for recombination of W^{20+} [4] and of W^{18+} [7]. The result of our partitioned damped theory agrees with the measured rate coefficient very well, considering the complexity of the theoretical problem and the simplifications which had to be applied.

Population modeling gives a (perhaps too) large upper limit (36%) for the metastable fraction present in the ion beam. However, calculation of the $\Delta n = 0$ contribution to DR from the lowest 16 initial levels does not give rise to a significant enough variation between them to justify any "correction" being applied to the measurement, nor does the overall comparison of totals between experiment and theory. This insensitivity of the recombination rate coefficient to the population of fine-structure excited initial levels is most probably a general phenomenon with complex ions where the density of multiply excited levels is large for all relevant symmetries.

Compared to the W^{19+} recombination rate coefficient from the ADAS database, our experimentally derived rate coefficient in a plasma is more than two orders of magnitude larger for temperatures up to 10 eV. At higher temperatures, in particular, in the range where W^{19+} is expected to exist in a collisionally ionized plasma, the discrepancy still amounts to factors of up to 20. Since this discrepancy is similar to what has been found previously for W^{20+} [4] we expect that recombination rate coefficients from the ADAS database are significantly in error also for tungsten ions of neighboring charge states.

[1] R. Pitts, S. Carpentier, F. Escourbiac, T. Hirai, V. Komarov, S. Lisgo, A. Kukushkin, A. Loarte, M. Merola, A. S. Naik, R. Mitteau, M. Sugihara, B. Bazylev, and P. Stangeby, J. Nucl. Mater. **438**, S48 (2013).

[2] S. P. Preval, N. R. Badnell, and M. G. O'Mullane, Phys. Rev. A **93**, 042703 (2016).

[3] S. D. Loch, J. A. Ludlow, M. S. Pindzola, A. D. Whiteford, and D. C. Griffin, Phys. Rev. A **72**, 052716 (2005).

[4] S. Schippers, D. Bernhardt, A. Müller, C. Krantz, M. Grieser, R. Repnow, A. Wolf, M. Lestinsky, M. Hahn, O. Novotný, and D. W. Savin, Phys. Rev. A **83**, 012711 (2011).

[5] N. R. Badnell, C. P. Ballance, D. C. Griffin, and M. O'Mullane, Phys. Rev. A **85**, 052716 (2012).

[6] C. Krantz, K. Spruck, N. R. Badnell, A. Becker, D. Bernhardt, M. Grieser, M. Hahn, O. Novotný, R. Repnow, D. W. Savin, A. Wolf, A. Müller, and S. Schippers, J. Phys.: Conf. Ser. **488**, 012051 (2014).

[7] K. Spruck, N. R. Badnell, C. Krantz, O. Novotný, A. Becker, D. Bernhardt, M. Grieser, M. Hahn, R. Repnow, D. W. Savin, A. Wolf, A. Müller, and S. Schippers, Phys. Rev. A **90**, 032715 (2014).

[8] ADAS, Atomic Data and Analysis Structure (2014), http://www.adas.ac.uk.

[9] V. A. Dzuba, V. V. Flambaum, G. F. Gribakin, and C. Harabati, Phys. Rev. A **86**, 022714 (2012).

[10] V. A. Dzuba, V. V. Flambaum, G. F. Gribakin, C. Harabati, and M. G. Kozlov, Phys. Rev. A **88**, 062713 (2013).

[11] A. Müller, Atoms **3**, 120 (2015).

[12] N. R. Badnell, Comput. Phys. Commun. **182**, 1528 (2011); http://amdpp.phys.strath.ac.uk/autos/.

[13] A. Kramida and T. Shirai, At. Data Nucl. Data Tables **95**, 305 (2009).

[14] M. Lestinsky, N. R. Badnell, D. Bernhardt, D. Bing, M. Grieser, M. Hahn, J. Hoffmann, B. Jordon-Thaden, C. Krantz, O. Novotný, D. A. Orlov, R. Repnow, A. Shornikov, A. Müller, S. Schippers, A. Wolf, and D. W. Savin, Astrophys. J. **758**, 40 (2012).

[15] G. Kilgus, D. Habs, D. Schwalm, A. Wolf, N. R. Badnell, and A. Müller, Phys. Rev. A **46**, 5730 (1992).

[16] S. Schippers, A. Müller, G. Gwinner, J. Linkemann, A. A. Saghiri, and A. Wolf, Astrophys. J. **555**, 1027 (2001).

[17] G. Gwinner, A. Hoffknecht, T. Bartsch, M. Beutelspacher, N. Eklöw, P. Glans, M. Grieser, S. Krohn, E. Lindroth, A. Müller, A. A. Saghiri, S. Schippers, U. Schramm, D. Schwalm, M. Tokman, G. Wissler, and A. Wolf, Phys. Rev. Lett. **84**, 4822 (2000).

[18] A. Foster, Ph.D. thesis, University of Strathclyde, 2008.

[19] T. Pütterich, Ph.D. thesis, University of Augsburg, 2005.

[20] A. Burgess, Astrophys. J. **141**, 1588 (1965).